

Balancing the Benefits of Vaccination: an *Envy-Free* Strategy.

Pedro Ribeiro de Almeida, Vitor Hirata Sanches, Carla Goldman

Instituto de Física - Universidade de São Paulo, CEP 05508-090, São Paulo-SP, Brasil.

June 2023

Abstract

The Covid-19 pandemic revealed the difficulties of vaccinating a population under the circumstances marked by urgency and limited availability of doses while balancing benefits associated with distinct guidelines satisfying specific ethical criteria (J.W.Wu, S.D. John, E.Y. Adashi, Allocating Vaccines in the Pandemic: The Ethical Dimension, The Am. J. of Medicine V.33(11): 1241 - 1242 (2020)). We offer a vaccination strategy that may be useful in this regard. It relies on the mathematical concept of envy-freeness. We consider finding balance by allocating the resource among individuals that seem to be heterogeneous concerning the direct and indirect benefits of vaccination, depending on age. The proposed strategy adapts a constructive approach in the literature based on Sperner's Lemma to point out an approximate division of doses guaranteeing that both benefits are optimized each time a batch becomes available. Applications using data about population age distributions from diverse countries suggest that, among other features, this strategy maintains the desired balance throughout the entire vaccination period.

Keywords: pandemic preparedness, balanced vaccine allocation, decision making process, envy-free division, direct and indirect benefits, Sperner's Lemma, cake-cutting.

1 Significance Statement

Direct and indirect benefits of vaccination are related to decreasing the severity of the individual's symptoms and to decreasing the spreading of the disease due to collective effects. The share with which a single dose contributes to each type of benefit may depend, among other conditions, on the age of the individual that receives it. This imposes difficulties in optimizing allocation guidelines that aim to support individual needs while controlling transmissibility. We offer a strategy of vaccination that may balance these two aspects based on the mathematical concept of envy-freeness. The present study revealed the efficiency of such a strategy and its tendency to equalize the benefits of vaccination locally, within a country, and among countries presenting the most diverse age distribution profiles.

2 Introduction

The unprecedented situation in which a vaccine was successfully developed amid the disease pandemic, the case of Covid-19, brought about urgent questions related to the possible strategies for allocation of the doses made available gradually in very small batches that do not cover the entire population in a community all at once [1], [2]. Given the high transmissibility of the virus and widespread infection, the problems associated with vaccine allocation highlighted the urgent need to elaborate and put in practice certain guidelines that best satisfy a given set of ethical requirements [3],[4]. In many countries, the prioritization followed protocols suggested by the WHO [1] to allocate the first doses that became available to the oldest and to those with comorbidities since these individuals are the most likely to develop severe forms of the disease [5], [6]. Other groups at maximum risk such as health care workers and, in some places, members of disadvantaged groups deprived of minimal protection against direct exposure to the virus, the homeless for instance, in addition to members of indigenous populations and isolated small communities, among others, have also been eligible for doses of the vaccine from the first batches [1].

It is worth noticing that, after the most elderly and other most-at-risk groups receive their doses, virtually the entire population remains unvaccinated while new doses continue to be available in very limited numbers. In the remaining susceptible individuals, comprising the large majority of the population, the ability to transmit the disease and the severity of the symptoms are widely dispersed, and these generally correlate with age. We restrict the contribution offered here to this scenario.

The elderly within this remaining population would still be mostly benefited directly from receiving the doses because they tend to develop the most severe forms of the disease compared to the younger that are likely to present with only mild symptoms, although this is not a rule [5]. On the other hand, due to their mobility and intense daily activity, younger people have a major capacity to transmit the virus compared to that of the elderly [3]. Therefore, vaccinating younger people would greatly benefit the entire population, as an indirect effect.

Direct and indirect effects of vaccination, regarding mainly the interplay between decreasing disease severity and its transmissibility, raise questions about the possibility of balancing these two factors that seem to compete with each other in making decisions about allocating vaccine doses [3]. We believe that any solution to this problem should comprise the following points: 1) a measure to evaluate proximity to a balanced condition that enables comparing results among different strategies of vaccination, and 2) a methodology to implement dose allocation that maintains such balance on time until vaccine coverage of the entire population is achieved.

We argue that this can be approached following an *envy-free* type of strategy for a fair division of doses among individuals possessing different utilities. The concept of envy-freeness is often illustrated in the literature by the classical cake-cutting problem [7], [8]. This refers to a partition among agents of a certain resource (the cake), generally heterogeneous, such that each one of the agents evaluates their parts as being the best among the parts chosen by the others. The heterogeneity of the resource is usually expressed through a utility function that assigns

to the different parts of the cake, different values satisfying additivity. In general, each agent has its own utility function. Here, we use the notion of utility to quantify both the direct and indirect benefits of vaccinating the diverse age groups of the population. We then formulate such a strategy to address the case of vaccine dose allocation by the agents to the individuals adapting the constructive approach presented in [9] and reviewed in [10] which is based on Sperner’s Lemma. For this, we assume that the vaccine is a desirable good and also that individuals and vaccine doses can be conceived as divisible quantities being represented by densities, defined appropriately. Accordingly, each age group receives a score named *utility* in agreement with the various views and plans of certain consultants or *counselors* expressing their priority criteria in line with the current public policies in the considered community.

We examine the case at issue regarding transmissibility and severity of the disease as a prototype to explain our ideas, although the model is not restricted to it. In keeping with this, it will be sufficient to consider the expertise of only two counselors, each one in charge of scoring all individuals according to their ages. One of the counselors referred to as C_A (Ana), is an expert in predicting the ways of spreading the disease. The other counselor, C_B (Bob), is an expert in disease symptomatology. Specifically, C_A represents the allocation guideline that accounts for the benefit of vaccinating to control transmission - the indirect effect of vaccination. C_B represents another allocation guideline that accounts for the benefit at the individual level - the direct effect of decreasing the severity of the symptoms. Both C_A and C_B are interested in balancing the two aspects; none of them wants to dispute vaccine doses. Therefore, whenever a new batch becomes available to this community, the doses will be allocated in such a way that each counselor agrees on the distinct groups of individuals to be vaccinated to optimize separately the benefit envisaged by each one. We claim that this characterizes an *envy-free* division of the vaccine doses.

The way that this may be accomplished is our main proposal and will be developed in the following Sections. We emphasize that unlike *utilitarian models* [11], [12], our strategy is not based on a single score system for which the priorities for doses allocation are evaluated in terms of the total score received by each individual from the different counselors. Rather, we conceive the model in such a way that each counselor optimizes the benefit according to their particular view. Our approach differs also from the *reserve system* strategies [13] for which the total vaccine supply from each batch is distributed according to pre-assigned proportions to certain reserved categories. In our model, the proportions of doses attributed to the management of each counselor are dynamic quantities, resolved along the process.

Our proposal is presented in Section 3. Illustrative examples are considered in Section 4. We compare the results from the application of the *envy-free* strategy using data comprised of certain population age distributions, with those predicted by the other two strategies examined, referred to as *oldest-first*, and *maximize-benefit*, as detailed below. We have also considered a strategy named *minimize-benefit* to set a scale to measure the efficiency with which the benefits are acquired by each strategy. These comparative results indicate that the *envy-free* leads to a considerable improvement in keeping the benefits related to C_A and C_B close together over time conferring support to this strategy as a way to pursue the desired balance. A discussion of these results and considerations about the

extent of the applicability of the model are presented in Section 5. In the Supplementary Material we outline the numerical procedure used to implement the model dynamically.

3 Model

Our formulation is decomposed into two parts. The first part consists of preliminary definitions to build up the relevant simplex as a basis for the choice of individuals to be vaccinated at each time. It is assembled using accessible data about population age distribution, taken in connection with the utility attributed to all groups of individuals by each counselor. The second part consists in building up the dynamics that drives this choice to achieve the required balance between the two guidelines.

3.1 The simplex

The age group distribution in a community with N susceptible individuals will be considered for the account of two counselors C_A and C_B , each one of them endowed with a utility function $\rho_\eta(I)$, $\eta = A, B$ hypothesized in such a way to attribute a score to each individual according to the corresponding age-related priority criteria. This can be performed by ordering these N individuals in such a way that their age $I(x)$ is a monotonic increasing surjective function of their positions $x \in \mathbb{Z} \cap [0, N]$.

In order to build up the *1-simplex* of interest over which we perform our considerations about the choices of the counselors, we map the interval $[0, N]$ into the interval $[0, 1]$ and variable x into a real variable $y = x/N$ such that $y \in [0, 1]$. The age at position y within this map shall now be calculated as $I(yN)$. We may assume that all individuals within the same age group are equally valued by each counselor though most likely, the value varies between counselors. It will be convenient though, to deal with continuous utility functions $\rho_\eta(I(yN)) \equiv \rho_\eta(y)$ represented by a combination of smoothed step functions for each counselor $\eta = A, B$, as detailed in Section 5. The *utility densities* $u_\eta(y)$ defined for all $y \in [0, 1]$ as

$$u_\eta(y) = \frac{\rho_\eta(y)}{\int_0^1 \rho_\eta(y) dy} \quad (1)$$

are the functions that allow for considerations about *envy-free* divisions based on Sperner's Lemma, as will be explained next. Observe also that any region ω of the considered simplex may be decomposed into a number M of disjoint sub-regions $\{v_j\}$, $j = 1, 2, \dots, M$. Each v_j , extended between endpoints y_{jI} (initial) and y_{jF} (final) with $y_{jI} < y_{jF}$, comprises a number $[(y_{jF} - y_{jI})N]$ of individuals, where the notation $[z]$ indicates the integer part of the real number z .

3.2 The dynamic

Consider a population that at a certain instant of time t comprises $N(t)$ susceptible individuals to whom a batch of $V < N$ vaccine doses shall be allocated. We suppose that the availability of the batches occurs at a certain frequency of $1/T$ until the entire population is vaccinated. We also assume that individuals achieve full protection after receiving a single dose. The time t shall then be better measured in terms of the interval T between batches as $t = nT$, for $n \in \mathbb{Z}_+$. The question posed here regards the choice of the V individuals to receive the doses at each time t in order to balance the current guidelines.

We think of two different priority criteria suggested by two *counselors* C_A and C_B expressing different opinions about how one should rank the population in the community to guide this choice. The *utility density functions* $u_A(y)$ and $u_B(y)$, $y \in [0, 1]$ conceived, respectively, by C_A and C_B assume nonnegative real values and represent a measure of the relevance for vaccinating the individuals ordered according to some rule. To present the methodology, we choose to order the individuals by their age, although this does not exclude any other possibility. Such an ordered list of individuals mapped into the interval $[0, 1]$ defines the *1-simplex* as detailed above. We aim to present a fair division strategy of an *envy-free* class through which the choice of the V individuals at each time balances the perspectives of the two counselors in the best possible way. The proposal offers an approximate solution extending the constructive approach [8] based on Sperner's Lemma as presented in [9] and reviewed in [10].

From the utility density functions $u_\eta(y)$, $\eta \in \{A, B\}$ we define the *benefit* $\mathcal{U}_\eta^{\omega(t)}$ according to the referred counselor perspective, that results from vaccinating the individuals inside a region $\omega(t)$ of the simplex at time t :

$$\mathcal{U}_\eta^{\omega(t)} \equiv \int_{\omega(t)} u_\eta(y) dy \quad (2)$$

The total benefit that is reached after vaccinating the entire population of susceptible amounts to one, according to both counselors:

$$\mathcal{U}_\eta = \int_0^1 u_\eta(y) dy = 1. \quad (3)$$

We proceed by partitioning the 1-simplex, at a time t , into a number d of identical parts, each of which comprised between a pair of neighbor points (p_i, p_{i+1}) at the positions $(y_{p_i}, y_{p_{i+1}})$, respectively, with $y_{p_j} = j/d$, for $j = \{0, 1, 2, \dots, d\}$. We then assign to the endpoint p_0 at $y_{p_0} = 0$ a label arbitrarily chosen between A and B so called in reference to the counselors, and then proceed by labeling each of the following points p_i of the sequence as A or B , alternately.

Observe that each point p_i at y_{p_i} splits the ordered population into two parts, part I on the left of p_i and part II on the right of p_i , comprising respectively N_I^i and N_{II}^i individuals at time t , such that

$$N_I^i = [y_{p_i} N] \quad (4)$$

$$N_{II}^i = [(1 - y_{p_i}) N]$$

At each of these points p_i we also consider splitting the batch of vaccines available at a certain time into two parts, V_I^i and V_{II}^i . We choose V_I^i and V_{II}^i proportional to N_I^i and N_{II}^i , respectively:

$$\begin{aligned} V_I^i &= [y_{p_i}V] \\ V_{II}^i &= [(1 - y_{p_i})V] \end{aligned} \tag{5}$$

To the extent that the simplex is arranged in this way, both quantities, i.e. individuals and vaccine doses, are evaluated using the single continuous variable y . This allows each counselor to express, at the corresponding labeled points p_i , what would be their preferential side to proceed with vaccination. We assume that V_I^i and V_{II}^i are intended necessarily to vaccinate individuals, respectively, on sides I and II defined for each i . Explicitly, to maximize benefit at each A -labeled point p_i , counselor C_A is asked to express her preference, based on u_A , about vaccinating V_I^i individuals on the side I or V_{II}^i individuals on the side II . The same for counselor C_B at each B -labeled point p_i , based on u_B . One should notice that it is implicit in this procedure, regardless of the counselors' choices, that neither of them would be able to vaccinate the entire population at once with the corresponding amount V_I^i or V_{II}^i of doses available on each side. Moreover, at an A -labeled point p_i where counselor C_A is in charge of choosing the side and decides for say, side II , she is supposed to make use of all of the V_{II}^i doses pre-assigned to that side. This implies that counselor C_B would necessarily vaccinate individuals on the other side using all of the V_I^i doses, even though it may not be his preferential's. Despite this, C_B would look for individuals amounting to V_I^i that are best to be vaccinated on the side I according to his utility density function. The same will be followed by counselor C_A after C_B has expressed his preferential choices at each B -labeled point p_i .

Accordingly, the counselor in charge at each point p_i , regardless of being labeled A or B , ends up vaccinating exclusively at one of the sides. Nonetheless, they would benefit from vaccination on both sides. Since both utility density functions assume nonzero values along the entire simplex, each counselor must account for a *benefit coupled* with the other's choice. In the example above we understand that, at that particular point p_i , counselor C_A has chosen side II and the best sub-region to vaccinate the V_{II}^i individuals at that side. This choice is foreseen after evaluating the total benefit from u_A composed of: (i) the amount obtained from u_A at a sub-region of II comprising V_{II}^i individuals that have been chosen according to her utility function u_A , and (ii) the *coupled benefit* that corresponds to the amount obtained from u_A at a sub-region of I comprising V_I^i individuals that have been chosen by suggestion of C_B , based on his utility density u_B . She concluded that the sum of (i) and (ii) is greater than the amount she would have obtained if she has chosen to vaccinate on the side I and received the coupled benefit from side II . For this, one must assume that both counselors know each other's utility density functions.

To extend (i) and (ii) to arbitrary choices, it will be useful to define for $\Gamma \in \{I, II\}$ and $\eta \in \{A, B\}$, the interval $\Omega_\eta^\Gamma(p_i, t)$, as the sub-region on the side Γ of the simplex with respect to point p_i where counselor η evaluates the maximum benefit from u_η at time t . According to this, counselor C_A looks for the largest between the *total benefit* $U_A^I(p_i)$ and $U_A^{II}(p_i)$ that, recalling (2), are defined as:

$$U_A^I(p_i, t) \equiv \mathcal{U}_A^{\Omega_A^I} + \mathcal{U}_A^{\Omega_B^{II}} \quad (6)$$

and

$$U_A^{II}(p_i, t) \equiv \mathcal{U}_A^{\Omega_A^{II}} + \mathcal{U}_A^{\Omega_B^I} \quad (7)$$

If $U_A^I(p_i, t) \geq U_A^{II}(p_i, t)$ she decides for side I , otherwise she decides for side II .

Likewise, to decide which side to vaccinate at each B -labeled point p_i , according to his utility function, counselor C_B looks for the largest between the *total benefit* $U_B^I(p_i, t)$ and $U_B^{II}(p_i, t)$, defined as:

$$U_B^I(p_i, t) \equiv \mathcal{U}_B^{\Omega_B^I} + \mathcal{U}_B^{\Omega_A^{II}} \quad (8)$$

and

$$U_B^{II}(p_i, t) \equiv \mathcal{U}_B^{\Omega_B^{II}} + \mathcal{U}_B^{\Omega_A^I} \quad (9)$$

If $U_B^{II}(p_i, t) \geq U_B^I(p_i, t)$ he decides for the side II , otherwise he decides for the side I .

The example discussed above corresponds to the case for which the pre-evaluation of the benefit by C_A , at the considered point p_i , resulted in $U_A^{II}(p_i, t) > U_A^I(p_i, t)$.

We finally observe that even though side I has no individuals to be vaccinated at the end-point p_0 at $y_{p_0} = 0$, the counselor in charge there might have two options: either to let the other vaccinate on side II using the entire amount V of doses, or to vaccinate the V individuals on side II . For example, if the point p_0 is A -labeled then counselor C_A will still be in charge to decide about her preferential side based on the largest between

$$U_A^I(p_0, t) = \mathcal{U}_A^{\Omega_B^{II}(p_0, t)}$$

and (10)

$$U_A^{II}(p_0, t) = \mathcal{U}_A^{\Omega_A^{II}(p_0, t)}$$

On the contrary, if the end-point p_0 is B -labeled then counselor C_B would select the side based on the largest between

$$U_B^I(p_0, t) = \mathcal{U}_B^{\Omega_A^{II}(p_0, t)}$$

and

(11)

$$U_B^{II}(p_0, t) = \mathcal{U}_B^{\Omega_B^{II}(p_0, t)}$$

Since at p_0 the values reached by u_A at $\Omega_A^{II}(p_0, t)$ are higher than or at least equal to the values reached by u_A at $\Omega_B^{II}(p_0, t)$ then $U_A^{II} \geq U_A^I$. Similarly, since the values reached by u_B at $\Omega_B^{II}(p_0, t)$ are higher than or at least equal to the values reached by u_B at $\Omega_A^{II}(p_0, t)$ then $U_B^{II} \geq U_B^I$. Therefore, the counselor in charge at p_0 will oneself prefer to indicate the individuals to be vaccinated, and this would happen on side II , instead of leaving vaccination up to the other counselor. Using similar arguments, one finds that for p_1 at $y_{p_1} = 1$ either one of the counselors would choose side I . Therefore, whoever counselor at p_0 , would choose the right side whereas whoever counselor at p_1 , would choose the left side. These conclusions assure that the conditions under which Sperner's Lemma holds are fully satisfied by the simplex defined above.

Finally, after the two counselors have expressed their preferential sides at each of the corresponding points p_i and the simplex looks like that sketched in **Figure 1** it allows one, through simple visual inspection, to list all pairs of consecutive points, referred here generically as (p_L, p_R) , such that the counselor at the point on the left p_L has expressed a preference to vaccinate on one of the sides say on side II , while the counselor at the point on the right p_R has expressed a preference to vaccinate on the opposite side, i.e. side I .

The existence of at least one such pair of points is ensured by Sperner's Lemma. Accordingly, for sufficient large partition d , an internal point p^* of the interval defined by any of these pairs will approximate a position at which the preferred sides of the two counselors are opposite to one another. The choice of any of those points p^* (if more than one) identifying opposite preferred sides for each counselor to allocate the available vaccine doses, characterizes an approximate *envy-free* division for which either

$$U_A^I(p^*) \geq U_A^{II}(p^*) \text{ and } U_B^{II}(p^*) \geq U_B^I(p^*) \quad (12)$$

or

$$U_A^I(p^*) \leq U_A^{II}(p^*) \text{ and } U_B^{II}(p^*) \leq U_B^I(p^*) \quad (13)$$

In order to carry on this strategy until all susceptible individuals in the population have the opportunity to get their doses, it is assumed that the procedure described above is repeated at each time t when a new batch containing V doses becomes available. For simplicity, we consider the unrealistic case for which V does not change along the entire process. On each of these occasions, the simplex must be re-scaled and the utility densities attributed

accordingly to the set of individuals mapped again into the interval $[0, 1]$, after excluding those already vaccinated with the doses from the previous batch.

We present a numerical study using this procedure for analyzing the time evolution of the benefit in selected population age distributions. The utility functions are written using an arbitrary scale to mimic counselors' general guidance. The results are compared with those produced by strategies specified in the following as *maximize-benefit*, *oldest-first* in addition to a *minimize-benefit* strategy introduced to set a scale for efficiency. The *maximize-benefit* strategy looks for distributing the doses to the groups of individuals for which the sum of the two utilities is maximized. The *minimize-benefit* strategy does the opposite. Under the *oldest-first* strategy, the doses available are fully distributed to the oldest individuals present at the time, approaching the current procedure adopted by many public health systems. Our findings are shown in the next Section.

4 Results

The time evolution of benefits acquired by applying each of the three strategies mentioned above is studied through numerical simulations. The methodology outlined (Supplementary Material) has been developed specifically to accomplish this. We use data for population age distribution of the countries indicated in [14]. For comparing the outcomes from the diverse strategies, the population of each country is divided into four age groups I_k , $k = 1, 2, 3, 4$, comprising, respectively, individuals from 0 to 14 years old (I_1), from 15 to 24 years old (I_2), from 25 to 64 years old (I_3), and those that are 65 years old or above (I_4). Any other division could have been considered. Before proceeding into the normalization, each counselor η assigns to each of these groups a utility value according to their particular priority criteria. Our choices are conceived using an arbitrary scale to set the quantities employed in the examples. These are indicated by the components of the vectors $\Psi_{(A)}^{(1)} = (12, 16, 4, 1)$ or $\Psi_{(A)}^{(2)} = (7, 23, 2, 1)$ for C_A , and $\Psi_{(B)}^{(1)} = (1, 4, 12, 16)$ or $\Psi_{(B)}^{(2)} = (1, 2, 7, 23)$ for C_B , which assume non-zero positive values and are independent of the number of individuals in each age group, characteristic of each community. These are then applied on Eq.(1) to build the utility density functions $u_\eta(y)$ for the diverse age distributions. We examine the four combinations: $\Psi_{(A)}^{(1)}$ and $\Psi_{(B)}^{(1)}$ (Default), $\Psi_{(A)}^{(1)}$ and $\Psi_{(B)}^{(2)}$ (Symptomatology.), $\Psi_{(A)}^{(2)}$ and $\Psi_{(B)}^{(1)}$ (Transmissibility), $\Psi_{(A)}^{(2)}$ and $\Psi_{(B)}^{(2)}$ (Concentrated). The idea is to test the choices of the counselors as the utilities become concentrated on the groups that each one of them finds the most priority to compare with the cases for which the utilities are less concentrated in a single group (Default). The utility density functions obtained using the population age distribution of the U.S. are shown in **Figure 2**. Analogous results have been obtained for the remaining countries (not shown). We emphasize that the assignments above for each $\Psi_{(\eta)}^{(1,2)}$ represent possible choices to compare the achievements of the different strategies and combinations of utilities considering the diverse age distributions. Any other possibility would be feasible, depending on the interests and attributions of the counselors.

Given $u_\eta(y)$ for each country and for each counselor, the simulated dynamic compares the outcomes using three

different strategies to allocate doses namely, *Envy-Free*, *Oldest-First*, and *Maximize-Benefit* one at the time, until vaccination ends.

Under *envy-free*, the preferred side of each of the two counselors at $p^*(t)$ are opposite to one another. Yet, because for a given η , $U_\eta^\Gamma(p^*)$ accounts also for the coupled benefits associated with the other's choice [6 - 9], the total region $\Omega(t)_{EF}$ to be vaccinated at each time t is necessarily composed of two or more disjoint segments spanned on both sides, the same for C_A and for C_B . That is, $\Omega(t)_{EF} = \Omega_A^I \cup \Omega_B^{II}$ if C_A preferred side I and C_B preferred side II , or $\Omega(t)_{EF} = \Omega_A^{II} \cup \Omega_B^I$ if C_A preferred side II and C_B preferred side I .

Under *oldest-first*, the focus is on the protection of the elderly. In this case, the choice of the fraction of individuals to be vaccinated with available doses is based exclusively on the distribution of the age groups. The preference is always for the V most elderly which fraction $v(t) = V/N(t)$ comprises a one segment region $\Omega(t)_{oldest}$ of the simplex at each time t . The *maximize-benefit* strategy, on the other hand, is based on the choice of the fraction $v(t)$ of individuals comprising a region $\Omega(t)_{max}$, eventually composed of disjoint regions, where the benefit achieved by adding the utilities from the two counselors is maximized.

Using definition (2), we express the average increment to the benefit achieved at time t as:

$$\mathcal{U}^{\Omega(t)} = \frac{1}{2}(\mathcal{U}_A^{\Omega(t)} + \mathcal{U}_B^{\Omega(t)}) \quad (14)$$

for all strategies, such that $\Omega(t) \in \{\Omega(t)_{EF}, \Omega(t)_{oldest}, \Omega(t)_{max}, \Omega(t)_{rand}\}$. These include a random vaccination process considered for comparison purposes, under which the fraction $v(t)$ of doses is offered to a randomly chosen fraction $\Omega(t)_{rand}$ of the simplex.

In all cases, the simulations run for an initial population comprising $N(0) = 10^4$ individuals and fixed vaccine batches of $V = 10^2$ doses each. The simplex built at every iteration time to follow the envy-free strategy was partitioned using $d = 100$ that ensures convergence of the results, as suggested by the study depicted in **Figure S2**. The whole procedure intends to find the regions $\Omega(t)$ to distribute the doses at each iteration time, that conform with each of the considered strategies. **Figures (3-7)** show results considering utilities combined as $\tau_{(A)}^{(1)}$ and $\tau_{(B)}^{(1)}$ (Default). The other combinations are also examined and the results are collected in **Figures (8-9)**. The time behavior of the increments $\mathcal{U}_A^{\Omega(t)}$, $\mathcal{U}_B^{\Omega(t)}$ and $\mathcal{U}^{\Omega(t)}$ in **Figure 3** are for the population of the U.S. All other distributions that we have examined exhibited the same patterns (results not shown). **Figure 4** exhibits the results for selected countries, as listed. Each point represents the time average of the differences (absolute values) $\overline{\Delta\mathcal{U}}$ between the increments to the benefit achieved by each of the two counselors,

$$\overline{\Delta\mathcal{U}} \equiv \frac{1}{\tau} \sum_{t=0}^{\tau} \left| \mathcal{U}_A^{\Omega(t)} - \mathcal{U}_B^{\Omega(t)} \right| \quad (15)$$

evaluated over the time interval τ encompassing the entire vaccination period, for the diverse strategies.

Figure 5 illustrates with the example of the U.S., the results obtained for the time evolution of the cumulative

benefits $\Phi_\eta(t)$:

$$\Phi_\eta(t) = \sum_{i=0}^t \mathcal{U}_\eta^{\Omega(i)} \quad (16)$$

for each of the two counselors $\eta = A, B$, and the mean:

$$\Phi(t) = \frac{1}{2}(\Phi_A(t) + \Phi_B(t)) \quad (17)$$

The outcomes obtained for all selected countries exhibited a similar pattern (results not shown).

Figure 6 depicts the time average of the differences (absolute values) between the contributions to the cumulative benefits of the two counselors, evaluated for all the countries listed:

$$\overline{\Delta\Phi} = \frac{1}{\tau} \sum_t |\Phi_A(t) - \Phi_B(t)| \quad (18)$$

Figure 7 shows the corresponding results for time average $\overline{\Phi}$ of $\Phi(t)$ (17):

$$\overline{\Phi} = \frac{1}{\tau} \sum_t \Phi(t) \quad (19)$$

These include the results for the minimize-benefit which is worth considering here precisely because it offers a lower bound to set a scale that allows one comparing outcomes, as we discuss next. **Figure 8** merges the results for the averages of cumulative benefits $\overline{\Delta\Phi}$ and $\overline{\Phi}$ using the considered strategies and combinations of utilities listed above extended for 236 countries (not specified).

5 Discussion and concluding remarks

The realistic case addressed here is that of deciding about strategies for allocating vaccine doses that become available to a community at a certain frequency but in very limited quantities. In the example used, we consider two guidelines to drive allocation. The first focuses on the direct benefit of decreasing the severity of the symptoms. The second focuses on the indirect benefit of decreasing transmission. We approach this situation by representing each of these guidelines as the priority of a qualified counselor in scoring the entire population ordered by age. Assuming that full protection of an individual is achieved after a single dose, the challenge is to select the group of individuals to be vaccinated every time a new batch becomes available to balance these two contributions. The difficulty relies on the fact that, in general, the amount by which a given vaccinated individual contributes to each of the benefits differ from each other. On the contrary, if both benefits were of the same magnitude, any strategy would result in a balanced condition. We claim that the strategy based on an *envy-free* division for dose allocation, as outlined above, offers a suitable and efficient choice to achieve such a balance in unpaired cases, as exemplified by the considered utilities. Our approach adapts the constructive analysis of the classic cake-cutting division problem [9] to conceive distributing doses optimizing the benefits envisaged by each counselor, which include the benefits coupled with the other's choice.

Consistent with this, the results in **Figure 3** of a case study certify that under the *envy-free* strategy, the increments to the benefit acquired at each time by each counselor remain very close together until vaccination is completed. Such results contrast with those obtained through *oldest-first* and *maximize-benefit* for which the increments to the two benefits differ considerably from each other across time. By adopting any of these two strategies, the selected regions of the simplex for doses allocation, either $\Omega = \Omega_{\text{oldest}}$ or $\Omega = \Omega_{\text{max}}$ along which $u_A(y)$ and $u_B(y)$ may assume very different values, leads to unbalanced $U_A^{\Omega(t)}$ and $U_B^{\Omega(t)}$. This is also the case with the random procedure. **Figure 4** suggests a measure $\overline{\Delta U}$ (15) for this imbalance averaged over time. The results for the diverse strategies are depicted for each of the selected countries. It shows that $\overline{\Delta U}$ approaches null values through the *envy-free* strategy. Relatively large values are obtained by applying the other two strategies and also by choosing the regions at random.

Although each of the benefits accumulates to the unity at the same time, the way that this is accomplished and the effects on the achievements of the two counselors can differ considerably. In this respect, the comparative results in **Figure 5** offer information about the efficiency with which the benefits evolve under different strategies. This can be better seen by interpreting cumulative data as the positions in time of the two particles in the space of benefits driven, each of them, by the corresponding counselor. Extending the analysis for the population age distributions of the selected countries, as shown, **Figure 6** depicts the average distance kept between these two particles in each case, until reaching their common final position simultaneously. Large values indicate that on average, one of the particles reached positions close to the goal considerably faster than the other. That is, for such strategies, the two benefits evolve out of sync over a considerably large period. This is the case for *maximize-benefit* and *oldest-first* in these examples. On the contrary, the positions of the two particles under the *envy-free* remain very close together at each instant through the entire time interval, suggesting that in addition to offering a way to promote a balance between acquired benefits, the strategy offers also a way to balance the instantaneous rates at which this happens. This is important for practical purposes since the intervals between consecutive batches may be very large, especially during the initial vaccination. The effects of a time delay between the achievements of each of the two benefits may have devastating consequences for the community. The random choice procedure offers balanced rates, on average, although the instant rates differ considerably since the sizes of the increments to the benefits alternate unbalanced.

Keeping with this kinematic interpretation, data in **Figure 7** refer to the time averages $\overline{\Phi}$ of the positions of the center of mass of the two particles achieved through the diverse strategies, and for all of the selected countries. The *maximize-benefit* presents the largest average value, as expected. Even though the partial benefits, i.e. the ones envisaged by each counselor, evolve at different rates in this case, both of them reach large values within relatively short times. *Envy-free* is also efficient in accumulating benefits almost as fast as the *maximize-benefit* does. Apparently, in all cases, the *oldest-first* and the random choice promote the worst results among all the considered procedures, except for a strategy introduced here named *minimize-benefit*. Under this, one looks for regions of the simplex that minimize the total benefit at each time. Although very implausible to be adopted in

practice, this strategy is useful to consider in the present analysis since it provides a lower bound to compare the efficiency of the diverse strategies investigated. Accordingly, the average benefit accumulated upon *envy-free* is much closer to the quantity accumulated by the *maximize-benefit* than that accumulated by the *minimize-benefit* (**Figure 7**). Random choice accumulates benefits at an average rate between the *maximize* and *minimize-benefit* strategies. The *oldest-first* spreads its contributions along the interval showing a strong dependence on the population age distribution.

Figure 8 depicts the results for (a) the time averages of the instantaneous difference $\overline{\Delta U}$ and (b) the time averages of the cumulative difference $\overline{\Delta \Phi}$, both against the average cumulative benefit $\overline{\Phi}$. Each point from a total of 236 composing a colored set, corresponds to the population distribution of a given country (not identified). The emphasis is given to the different combinations of utilities and strategies employed. In all cases, the results are in line with the behavior depicted in **Figures 4, 6, and 7**, for the utility pair named Default. The *envy-free* strategy is unique in achieving the smallest differences $\overline{\Delta U}$ and $\overline{\Delta \Phi}$ among all strategies and in producing total benefit at a rate that, on average, is the closest to that achieved by *maximize-benefit*. Although the *maximize-benefit* (and in parallel, the *minimize-benefit*) approaches the results for the *envy-free* regarding the cumulative difference $\overline{\Delta \Phi}$, the dispersion of data increases considerably in these cases. A surprising outcome from the study in **Figure 8** is that the *envy-free* reveals a tendency to minimize the dispersion of the distributions for both $\overline{\Delta \Phi}$ and $\overline{\Phi}$ when compared to the corresponding results achieved by the other strategies. For all pairs of utilities chosen, the remaining strategies produced large dispersion either for $\overline{\Delta \Phi}$ or $\overline{\Phi}$, or for both. Collectively, these results indicate that among all of the considered strategies the *envy-free* promotes a good balance between the benefits envisaged by the two counselors over time, and also that this happens at similar and relatively high rates at initial times resulting in fast accumulation of benefits. In addition, it is the strategy that tends to equalize the benefits of vaccination among diverse countries, which is desirable within a scenario of a pandemic. We thus believe that the proposed strategy fulfills the requirements stated in the introduction since it maintains the balance in agreement to different measures comprising a) the amount of benefit acquired at each time by each counselor, b) the efficiency of the process given the speed with which the cumulative benefit approaches limiting values, and c) the tendency to equalize the effects achieved by distinct population age distributions.

We have assumed throughout that the only mechanism by which individuals are removed from the simplex is through vaccination. We do not account for varying vaccine efficacy or deaths, whether caused by the disease or by any other reason across the vaccination period. Once the two counselors provide the utilities, we predict the fraction of individuals from each age group, and at each time, that should be vaccinated to guarantee the balance. The results in **Figure 9** exemplify in the case of the U.S. the kind of outcome provided by each of the four combinations of utilities, as indicated. In all cases, individuals of 65+ and those comprised within 15 – 24 years old are indicated to be prioritized across the initial batches.

The effects of vaccine efficacy have been considered in previous studies using optimization algorithms [15], [16] in

connection to the evolution of age-stratified population models. In particular, an SEIR (susceptible, exposed, infectious, recovered) model dynamics has been considered for analyzing different scenarios for the choice of the age groups at the initial period of vaccination [17]. Given the proposal developed here, it might be interesting to conceive a vaccination plan based on an interplay between the dynamic of the envy-free and that of the SEIR model. Such a protocol would be able to minimize morbidity while balancing benefits.

Finally, it should emphasize that the model offered here is not in any possible way restricted to the specific guidelines addressed above. These have been selected as references to explain and illustrate the practice of the method. Any other guideline could have been chosen to drive the allocation of available units. In addition, because Sperner's Lemma can be extended to more dimensions [9], [10], this opens the possibility to extend the constructive strategy described above to approach more realistic situations in which there are more than two guidelines defining priorities [3]. We believe that this offers an attractive perspective to resolve such complex problems, with the help of careful and skilled counselors.

Supplementary Material

Methods

Here, we sketch the algorithm we have developed to find the envy-free division for vaccine allocation, given a pair of utility density functions.

The time $t = nT$ of the n^{th} iteration is measured in intervals $T = 1$ between the availability of consecutive vaccine batches with V doses each. A fraction $v(t) = V/N(t)$ from the simplex embracing $N(t) > V$ susceptible individuals at t is selected for vaccination and then, removed. The simplex must then be re-scaled in order to map the remaining $N(t+1) = N(t) - V$ susceptible into the interval $[0, 1]$ to resume the process of vaccination at the time $t+1$. Therefore, each iteration of the simulation comprises three steps: a decision step; a removal step; and a re-scaling step, which are sketched in **Figure S1**.

Decision Step

This is the part that distinguishes the strategies to drive vaccination. To proceed with the *envy-free*, we follow the procedure detailed in Section 3 to build the simplex, label it, and use Equations (6 - 9) to determine which side each counselor would choose to vaccinate at each labeled point. Then, by inspection, we identify all pairs of points (p_L, p_R) between which an *envy-free* point $p^*(t)$ must be located. We choose the average positions between p_L and p_R to approximate the actual $p^*(t)$ at each time. The structure of the simplex with the continuous functions $\rho^{(\eta)}(y)$ to approach the utility densities of counselor $\eta = A, B$, guarantees the existence of at least one *envy-free* point between each pair (p_L, p_R) .

To build up such a function we suppose that a value $\psi_k^{(\eta)}$ is attributed by counselor η to each age group labeled $k \in \{1, \dots, m\}$, that decompose the population of the interval $[0, 1]$ into m sub-intervals, each of these enclosed between initial and final points, respectively y_k^I and y_k^F , for all k . Continuity at the frontiers between neighboring sub-intervals is assured by means of Sigmoid functions with an additional parameter B coinciding with the slope at the origin:

$$G(y) = \frac{1}{1 + e^{-By}}. \quad (\text{S1})$$

This allows a construction of the functions $\rho^{(\eta)}(y)$ as

$$\rho^{(\eta)}(y) = \psi_1^{(\eta)} [1 - G(y - y_1^F)] + \sum_{k=1}^{m-1} \psi_k^{(\eta)} [G(y - y_k^I) - G(y - y_k^F)] + \psi_m^{(\eta)} [G(y - y_m^I)] \quad (\text{S2})$$

The normalized utility density functions $u^{(\eta)}(y)$ defined by equation (1) for each η are evaluated for $\rho^{(\eta)}(y)$ defined above.

A remark is in order here regarding an eventual identification of several *envy-free* points in the simplex, at each time t . When this is the case, we proceed by choosing the one leading to the smallest difference between the benefits envisaged by the two counselors. In case of a tie, we choose the *envy-free* point leading to the greatest benefit resulting from adding the two contributions. If the simplex would still present more than one *envy-free* point, we select one of them randomly.

Removal Step

The choice of an *envy-free* point at the Decision Step prescribes a set Λ of $L(t)$ intervals $\Lambda = \{\lambda_1(t), \dots, \lambda_{L(t)}(t)\}$ $\lambda_l(t) \in [0, 1]$, each one of them selected either by C_A or by C_B to maximize each one benefit, accounting for the coupled contribution from the other's choice. The union of all $\lambda_l(t)$, $l \in \{1, \dots, L(t)\}$, corresponds to the fraction $v(t) = V/N(t)$ of the population vaccinated at time t which is then removed from the interval $[0, 1]$. At the end of this removal process occurring at the interaction time t , the simplex turns out into a set of $L(t) + 1$ disjoint intervals $s_j(t) = [s_j^I(t), s_j^F(t)]$, $j \in \{1, \dots, L(t) + 1\}$ which union

$$S(t) = \bigcup_j s_j(t) \subseteq [0, 1] \quad (\text{S3})$$

shall be re-scaled to define the simplex at the time $t + 1$. The construction is sketched in **Figure S1** for $L = 2$.

Re-scaling Step

After removing the individuals vaccinated at time t , each interval $s_j(t)$ is re-scaled into a new interval referred to as $\zeta_j(t + 1)$. The union of all $\zeta_j(t + 1)$ defines the new simplex $[0, 1]$ over which the former steps shall be repeated at time $t + 1$:

$$Z(t + 1) = \bigcup_j \zeta_j(t + 1) = [0, 1] \quad (\text{S4})$$

The intervals $\zeta_j(t + 1)$ are set through the scale factor

$$r(t; t + 1) = \frac{N(t)}{N(t + 1)} = \frac{1}{(1 - v(t))} \quad (\text{S5})$$

so that the first interval $\zeta_1(t + 1)$ has its endpoints calculated as:

$$\zeta_1^I(t + 1) = 0 \quad (\text{S6})$$

$$\zeta_1^F(t + 1) = \Delta s_1(t) r(t; t + 1)$$

where $\Delta s_j(t) = s_j^F(t) - s_j^I(t)$ is the size of the interval $s_j(t)$. The remaining intervals $[\zeta_j^I(t+1), \zeta_j^F(t+1)]$ for all $j > 1$ are set as:

$$\zeta_j^I(t+1) = \zeta_{j-1}^F(t+1) \tag{S7}$$

$$\zeta_j^F(t+1) = \zeta_j^I(t+1) + \Delta s_j(t)r(t; t+1)$$

$Z(t+1)$ defines the simplex that will be considered in the next iteration, at the time $t+1$. The three steps described above are iterated up to the vaccination is completed.

About the choice of parameter d

Sperner's Lemma guarantees that the envy-free strategy will always find at least one pair of points (p_L, p_R) enclosing an envy-free point p^* at the end of each iteration time. However, if the considered number d of divisions of the simplex is too small, the average between these two points may not be a good approximation to p^* , as we have assumed. In this case, changing d may lead to oscillations in the value of p^* and, most probably, in the quantities derived from it. Improving the approximation by increasing d is expected to reduce such oscillations as p^* approaches its actual value. This, however, implies adding considerable computational costs to the numerical procedure. To achieve a compromise between mathematical accuracy and computational performance in this case, we examine how the change in d directly affects the temporal averages of the quantities shown in **figures 4, 6, and 7** using as an example, the population age distribution from the U.S.. **Figure S2(a)** shows the average temporal behavior of the difference of the benefits (absolute values) ((15)) due to the contributions of the two counselors obtained through the envy-free strategy, as d increases. **Figure S2(b)** shows the corresponding behavior of the cumulative differences (18), and **Figure S2(c)** shows the mean cumulative benefit (19). As expected, the amounts oscillate around the mean until stabilizing at a certain value of d that is not the same for the different quantities analyzed. We proceed into the whole numerical calculation presented above choosing $d = 100$ which seems suitable to ensure convergence of the results in all cases.

Other strategies

The other strategies considered to simulate the dynamics of vaccination, in particular the *maximize benefit* and the *oldest-first*, introduce changes into the Decision Step described above.

The *maximize-benefit*, is based on the choice of the region $\Omega(t)_{\max}$ in the simplex which is of the size of the total fraction $v(t) = V/N(t)$ of individuals to be vaccinated at each time t , such that it maximizes the total benefit, accounting for both counselors according to the prescription in (14) for $\Omega(t) = \Omega(t)_{\max}$. The iterating procedure follows then the same removal and re-scaling steps as for the *envy-free*.

The implementation of the *oldest-first* strategy consists in allocating the total fraction $v(t) = V/N(t)$ of vaccine doses available at the time t to the oldest fraction of the population present at that time. The resulting benefit is evaluated according to (14) for $\Omega(t) = \Omega(t)_{\text{oldest}}$. The iterating procedure follows then the same removal and re-scaling steps as for the *envy-free*.

Acknowledgements

The authors acknowledge D.H.U. Marchetti for comments and suggestions on the manuscript. P.R.A acknowledges the financial support from the Brazilian agency Coordenação de Aperfeiçoamento de Pessoal de Nível Superior (CAPES).

References

- [1] World Health Organization, A Global Framework to Ensure Equitable and Fair Allocation of COVID-19 Products and Potential implications for COVID-19 Vaccines, 18 June 2020; <https://bit.ly/https://1drv.ms/u/s!ApaXW-xuBujRqF60FeJAdKSCkWMC?e=3eSf7Q/32rhHPb>.
- [2] H.Gayle, A Framework for Equitable Allocation of COVID-19 Vaccine, National Academy of Sciences, Engineering and Medicine 2020, Washington, DC: The National Academies Press. <https://doi.org/10.17226/25917>.
- [3] J.W.Wu, S.D. John, E.Y. Adashi, Allocating Vaccines in the Pandemic: The Ethical Dimension, The Am. J. of Medicine V.33(11): 1241 - 1242 (2020).
- [4] Ezekiel J. Emanuel, Govind Persad, Adam Kern, Allen Buchanan, Cécile Fabre, Daniel Halliday, Joseph Heath, Lisa Herzog, R. J. Leland, Ephrem T. Lemango, Florencia Luna, Matthew S. McCoy, Ole F. Norheim, Trygve Ottersen, G. Owen Schaefer, Kok-Chor Tan, Christopher Heath Wellman, Jonathan Wolff, Henry S. Richardson, An ethical framework for global vaccine allocation, Science 369(6509): 1309-1312 (2020).
- [5] Kai Liua, Ying Chenb, Ruzheng Linc Kunyuan Han, Clinical features of COVID-19 in elderly patients: A comparison with young and middle-aged patients, J. of Infection 80: e14–e18 (2020).
- [6] Huang C, Wang Y, Li X, Ren L, Zhao J, Hu Y, Zhang L, Fan G, Xu J, Gu X, Cheng Z, Yu T, Xia J, Wei Y, Wu W, Xie X, Yin W, Li H, Liu M, Xiao Y, Gao H, Guo L, Xie J, Wang G, Jiang R, Gao Z, Jin Q, Wang J, Cao B Clinical features of patients infected with 2019 novel coronavirus in Wuhan, China. Lancet. 395(10223): 497 (2020).
- [7] L. E. Dubins and E. H. Spanier, How to Cut A Cake Fairly, The American Mathematical Monthly 68(1): 1- 17 (1961).

- [8] S. J. Brams, A. D. Taylor, An Envy-Free Cake Division Protocol, *The American Mathematical Monthly*, 102(1): 9-18 (1995).
- [9] F.E. Su, Rental harmony: Sperner's lemma in fair division. *Am. Math. Monthly* 106, 930–942 (1999).
- [10] M. DeVos. D.A. Kent, *Game Theory - a Playful Introduction*, Am. Math. Soc., Student Math. Library V. 80, Providence, Rhode Island (2016).
- [11] D.B.White , M.H. Katz, J.M. Luce, B. Lo, Who should receive life support during a public health emergency? Using ethical principles to improve allocation decisions. *Ann. Intern. Med.* 150(2): 132-138 (2009).
- [12] Y. Liu, S. Salwi S, B.C. Drolet, Multivalued ethical framework for fair global allocation of a COVID-19 vaccine. *J Med Ethics* 46(8): 499-501 (2020).
- [13] A.T. Makhoul, B.C. Drolet, A Reserve System for the Equitable Allocation of a Severe Acute Respiratory Syndrome Coronavirus 2 Vaccine, *Chest* 159(3): 1292 - 1293 (2021).
- [14] <https://population.un.org/wpp/Download/Standard/MostUsed/>; United Nations, Department of Economic and Social Affairs, Population Division (2022). *World Population Prospects 2022*, Online Edition.
- [15] L. Matrajt, J. Eaton, T. Leung, E. R. Brown, Vaccine optimization for COVID-19: Who to vaccinate first? *Sci. Adv.* 7(6) : eabf1374 (2021).
- [16] J.H. Buckner, G. Chowell, Michael R. Springborn, Dynamic prioritization of COVID-19 vaccines when social distancing is limited for essential workers, *Proc. Nat. Acad. Sci. USA*, Vol. 118(16) e2025786118 (2021).
- [17] K. M. Bubar, K. Reinholt, S. M. Kissler, M. Lipsitch, S. Cobey, Y. H. Grad, D. B. Larremore, Model-informed COVID-19 vaccine prioritization, *Science* (371): 916–921 (2021).

Legends

- **Figure 1** - A labeled simplex defined by a partition with $d = 9$. The scheme follows Ref. [10] to illustrate in the present case possible choices of counselors C_A , at points A and C_B , at points B , about vaccinating on side I or on side II . Each of the regions between an identified pair (p_L, p_R) encloses a point p^* that sets an envy-free division of the simplex.
- **Figure 2** - Illustrative example. Utility density functions evaluated by each counselor C_A (purple) and C_B (green) considering the four combinations of utilities, as indicated, for the population age-groups of the U.S.
- **Figure 3** - Simulated time series for the benefits (2) acquired by each counselor, C_A (orange) and C_B (blue) through (a) a random procedure and strategies (b) *maximize-benefit*, (c) *oldest-first*, (d) *envy-free*. The utility density functions employed correspond to the combination defined as Default in Fig.(2) and the results shown are for the population age-distribution of the U.S.
- **Figure 4** - Time average of the differences (absolute values) (15) between the contributions of the two counselors to the benefits obtained through each strategy, extended to the population age-groups of the selected countries, as specified. The utility density functions employed correspond to the combination defined as Default.
- **Figure 5** - Simulated time series for the cumulative benefits $\Phi_\eta(t)$ (16) acquired by each counselor, C_A (orange) and C_B (blue) through (a) a random procedure and strategies (b) *maximize-benefit*, (c) *oldest-first*, (d) *envy-free*. The utility density functions employed correspond to the combination defined as Default in Fig.(2). The results shown are for the population age-distribution of the U.S.
- **Figure 6** - Time average of the differences (absolute values) $\overline{\Delta\Phi}$ (18) between the contributions of the two counselors to the cumulative benefits obtained through each strategy, extended to the population age-distributions of the selected countries, as specified. The utility density functions employed correspond to the combination defined as Default.
- **Figure 7** - Time average of the mean cumulative benefit $\overline{\Phi}$ (19) between the contributions of the two counselors, for each strategy and selected countries. The utility density functions employed correspond to the combination defined as Default.
- **Figure 8** - Time averages of (a) the cumulative differences (absolute values) $\overline{\Delta\Phi}$ (18), and (b) the instantaneous differences (absolute values) $\overline{\Delta U}$ (15) against the mean $\overline{\Phi}$ (19), evaluated for the population age-distributions of 236 selected countries for strategies and utility combinations, as indicated by colors. The distributions of the points are indicated by the lateral diagrams. *Maximize-benefit* (blue) *minimize-benefit* (green), *oldest-first* (brown), *envy-free* (red) and random procedure (orange).

- **Figure 9** - Indication of the population fraction per age group to receive the doses at each time to follow the *envy-free* strategy considering the different combinations of utilities, as indicated. The results shown are for the population age-distribution of the U.S.
- **Figure S1** - Schematic view of a model simplex at an iteration time t . (1) An envy-free division point p^* is identified. (2) The regions λ_1 and λ_2 corresponding to the fractions of individuals that received the doses are removed from the simplex. (3) The remaining regions s_1 , s_2 , and s_3 are reset through the scale factor r to recompose the simplex for the analysis at time $t + 1$.
- **Figure S2** - Study of convergence of the results as d varies. The quantities examined are indicated on the axis. In each case, the median is indicated by the orange line.

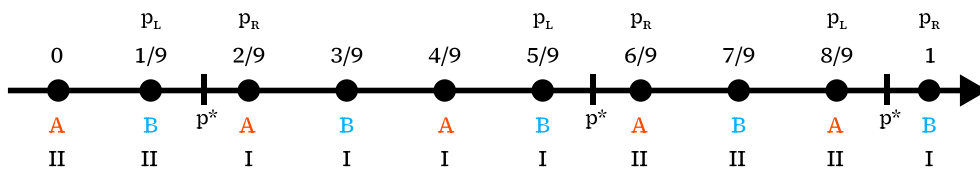


Figure 1

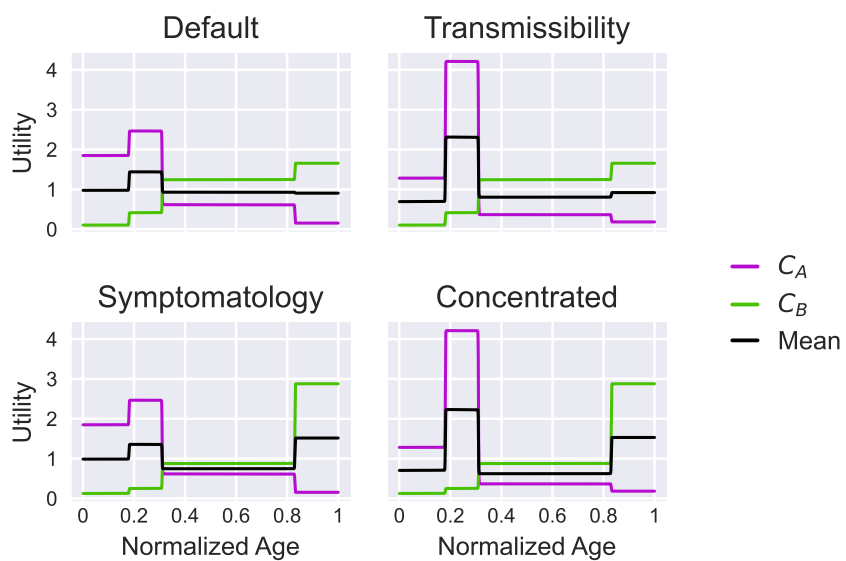


Figure 2

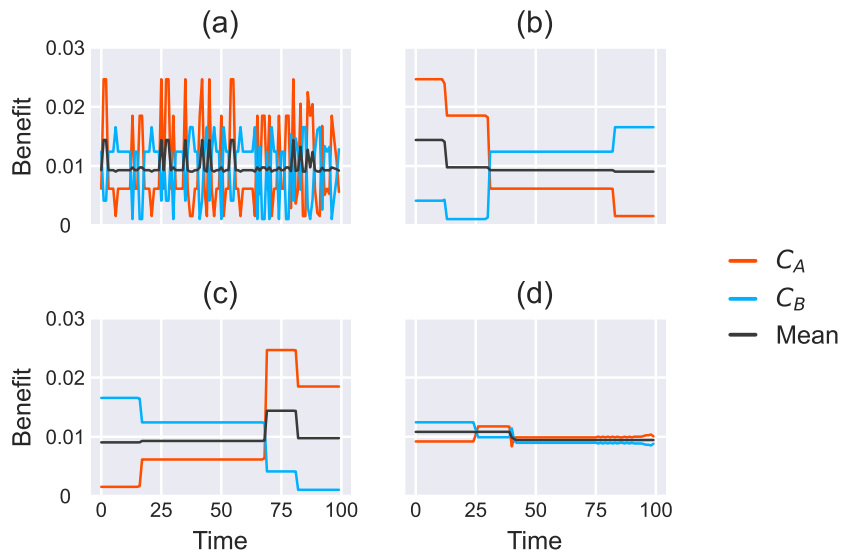


Figure 3

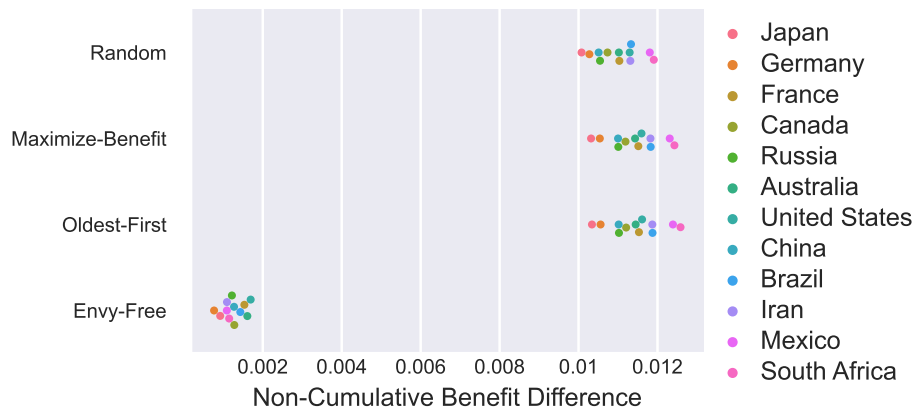


Figure 4

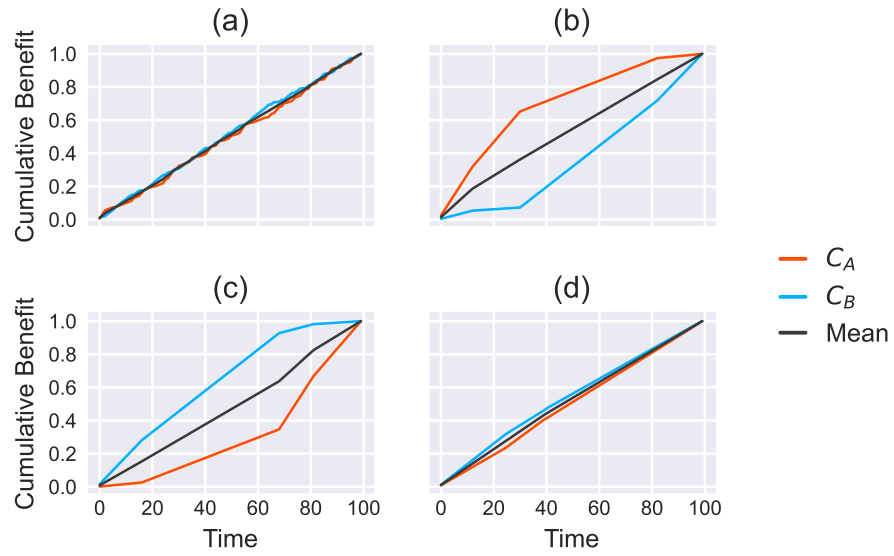


Figure 5

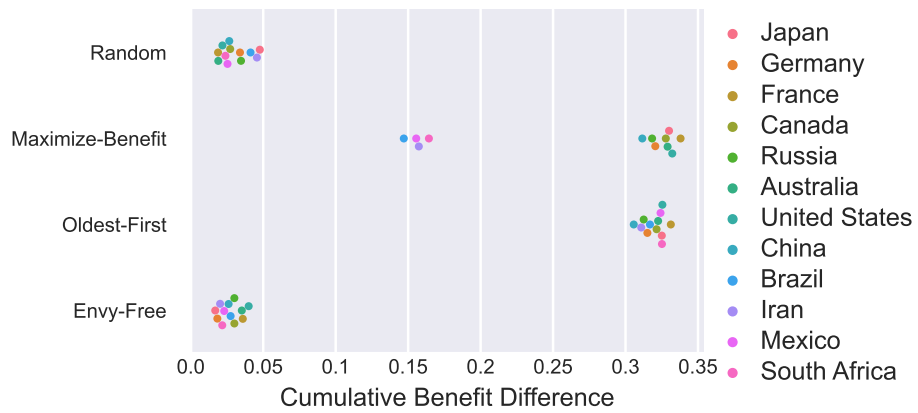


Figure 6

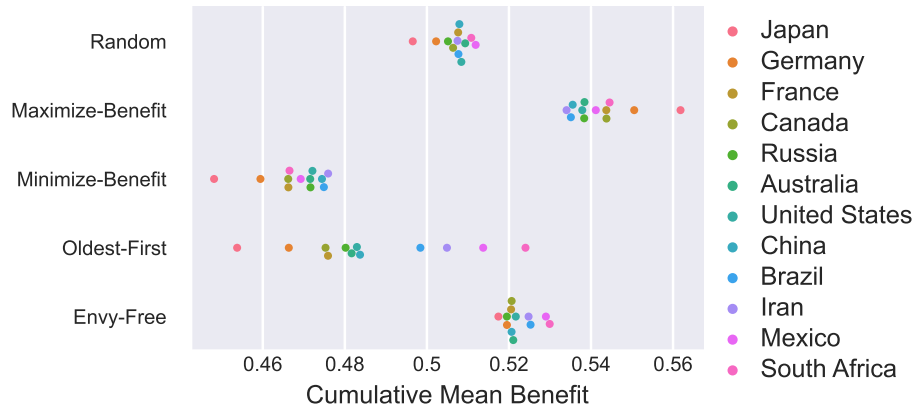


Figure 7

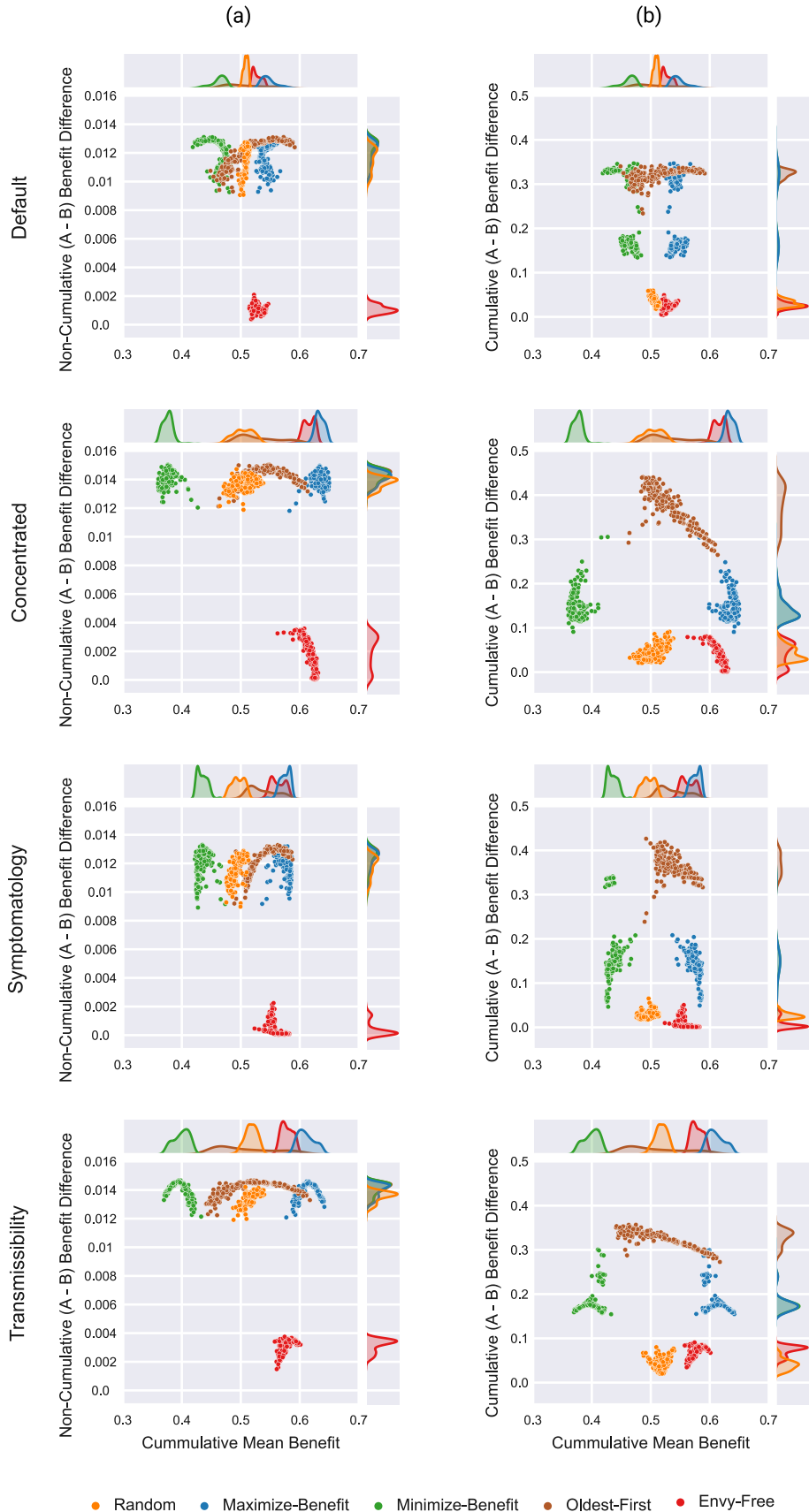


Figure 8
26

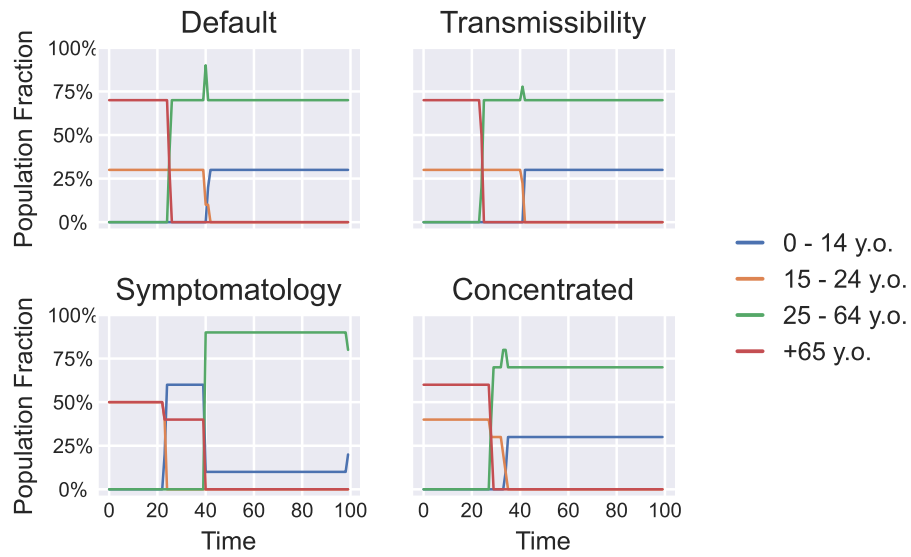


Figure 9

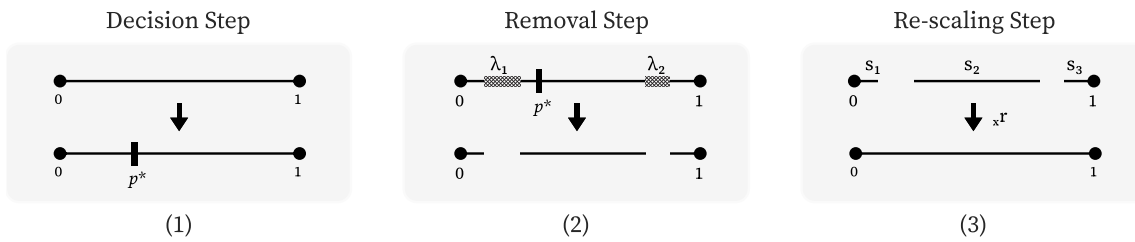


Figure S1

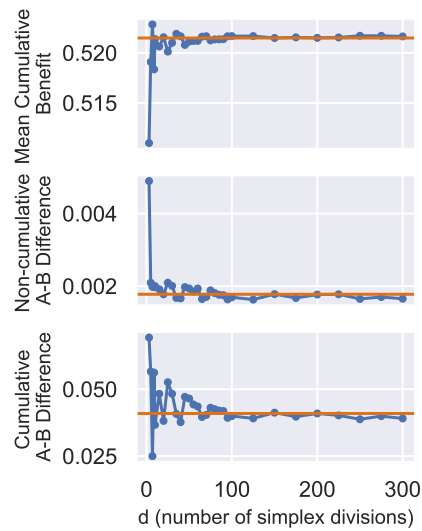


Figure S2